JOURNAL OF MATERIALS SCIENCE **39** (2004) 433–443

Morphology-tensile behavior relationship in injection molded poly(ethylene terephthalate)/polyethylene and polycarbonate/polyethylene blends (II)

Part II *Tensile behavior*

ZHONG-MING LI, BANG-HU XIE
College of Polymer Science and Engineering, State Key Laboratory of Polymer Materials Engineering, Sichuan University, Chengdu, 610065, Sichuan, People's Republic of China

SHUYING YANG
Mechanical Engineering Department, University of Texas Pan America, Edinburg, TX 78541, USA

RUI HUANG, MING-BO YANG*
College of Polymer Science and Engineering, State Key Laboratory of Polymer Materials Engineering, Sichuan University, Chengdu, 610065, Sichuan, People's Republic of China
E-mail: yangmb@scu.edu.cn

The tensile behavior of injection molded poly(ethylene terephthalate) (PET)/polyethylene (PE) and polycarbonate (PC)/PE blends was investigated. For the same blend, due to the difference in the elongated dispersed particle concentration, the specimens molded at higher injection speed had slightly higher tensile strength and modulus than those molded at lower speed. Moreover, the reinforcement effect of PC to PE matrix was more noticeable than PET to PE. For the stress-strain behavior, while the PET/PE blend behaved like a common injection-molded immiscible blend the PC/PE blend unusually underwent twice yielding regardless of the cross head speed. For the PET/PE blend, obvious debonding between the dispersed PET particles and the matrix PE occurred upon elongation, resulting in large grooves and voids behind the particles. The PET particles experienced slight plastic deformation from spheres to ellipsoids. The stress whitening first appeared in the necking zone then extended along cold drawing zone. For the PC/PE blend, the PC particles in the core layer experienced considerable plastic deformation throughout the tensile test. Consequently, most of PC particles in the fractured specimen were deformed into fibers. Owing to comparatively high amount of injection-induced fibers that distributed or transferred the external stress, the specimen of PC/PE blend first deformed evenly in the entire tested zone, characterized by stress whitening in the entire specimen. Then after the first yielding, the stress decreased slowly while the elongation continued. When the elongation reached a certain point, the fibers in the sub-skin layer could no longer endure the external stress, and accordingly the second yield took place. Additionally, the fibrillation of the spherical PC particles in the core layer appeared right after the second yielding point.

1. Introduction

It is well known that morphology dominates mechanical properties of a plastic part to a great degree, hence the investigation of the morphology-property relationship is a long term subject [1–10]. The injection molding is a most commonly used processing operation in the plastics industry. It is also one of the most complicated processing operations, that imparts high stress and rapid cooling as the polymers are formed into useful shapes [3]. Especially for immiscible polymer blends, under both strong stress field and non-isothermal field during injection molding, the deformable minor phase can be deformed *in situ* into a variety of morphological structures such as spheres,

*Author to whom all correspondence should be addressed.

ellipsoids, fibers, and plates [12–20]. Additionally, the microstructure is unevenly distributed in the injection-molded parts, displaying an anisotropic morphology, termed skin-core structure [20–28]. This leads to more difficulty in revealing the influences of the morphology on the mechanical properties of the injection molded blends. Generally, limited attention has been paid to the phase morphology and the mechanical properties of injection-molded immiscible blends compared to miscible polymer blends [10, 14, 22]. Karger-Kocsis [1] is one of the earliest researchers to systemically study this subject. He explored the structure-property relationship as well as the failure phenomenon of injection molded polypropylene blends modified with ethylene/propylene/diene terpolymer and thermoplastic polyolefin rubber. It was found that during injection molding, a skin-core morphology was formed in both the continuous PP matrix as well as in the modified PP blends containing rubber particles of various deformation. It was claimed that failure during tensile and tensile impact loading is initiated in the shear zone along the skin-core boundary. The final failure mode of the injection-molded blends depends the interaction of crazing and shear yielding. Recently, Karger-Kocsis and Mouzakis [16] studied the effect of the injection-molding induced skin-core morphology on the behavior of rubber-toughened polypropylene (RTPP) systems by using the essential work of facture method. RTPP with high ethylene/propylene rubber (EPR) showed no skin-core structure after molding and the EWF approach worked well in this case. In contrast, RTPP with low EPR exhibited a pronounced skin-core morphology: EPR depletion and enrichment were observed in the skin and core region, respectively. This morphology caused necking instead of crack growth in deeply double edge-notched specimens under tensile loading along the mold filling direction. The necking process not only was accompanied by a large scatter but also yielded highly unrealistic specific essential work of fracture values. Guerrica-Echevarria *et al*. [17] studied phase behavior and physical properties of injection-molded polyamide 6/phenoxy blends. SEM showed biphasic structures with slightly elongated dispersed phases in tensile specimens before testing that, unlike impact specimens, became fibrillar after tensile testing. These oriented structures appeared to be the main reason for the observed additive ductility values, in spite of the immiscibility.

In paper I [29], the morphology of injection molded poly(ethylene terephthalate) (PET)/polyethylene (PE) and polycarbonate (PC)/PE blends is discussed. The mold used was a single-gate mold. The results indicate that both shape and size of the PET and PC phases depended not only on the nature properties of PET/PE and PC/PE blends, but also on the injection molding parameters like injection speed as well as the position throughout the entire molded bar. The morphology in the section perpendicular to the melt flow direction included four layers: surface, sub-skin, and intermediate layers as well as core zone. The sub-skin layer contained more or less fibrous structure and its thickness gradually decreased along the molded bar from gate toward non-gate end. At the same injection speed, the amount of injection-induced fibers in PC/PE is much higher than that in the PET/PE blend. In the core region, the dispersed phase is mainly spherical particles whose diameter increased along the melt flow pathway. Between these two layers, there is an intermediate layer where the dispersed particles mainly assumed the form of fibers, ellipsoids or spheres. Generally, the diameter of PET particles is larger than PC ones no matter whether the dispersed particles are elongated or not during injection molding.

The objective of this study is to investigate the influences of injection-induced morphology of PET/PE and PC/PE blends on the tensile behavior of the injection molded blend bars, emphasizing the differences between the two. We choose PET/PE and PC/PE blends because PET/PE is a typical semicrystalline/semicrystalline polymer system with a viscosity ratio less than unity, and PC/PE a typical amorphous /semicrystalline polymer system with a viscosity ratio higher than unity.

2. Experimental

2.1. Materials and preparation of test pieces

The materials and their properties, including the number molecular weight, are summarized in paper I [29]. Details of the injection molding conditions are also given in paper I [29].

2.2. Tensile testing

The tensile tests were performed at room temperature according to ASTM D-638 using the dog-bone specimens. The distance between the grips was 100 mm as recommended in the standard. The crosshead speed of the apparatus varied from 30 to 300 mm/min while the strain was determined on a 50 mm length zone in the middle part of the specimens by an extensometer. Tensile modulus was determined at a strain of 1%. Photos of some stretched specimens were taken by a digital camera to compare the macroscopic morphology evolution of PET/PE and PC/PE blends.

2.3. Morphological observation

Electron microscopic observation of the specimens after the tensile testing was performed on a JEOL JSM-5900LV scanning electron microscope (SEM). The specimens were frozen in liquid nitrogen for one hour, then cut along the drawing direction in the necking zone with a fresh razor to make surfaces for observation. The surfaces were covered with a layer of gold to make them conductive prior to examination. In order to examine the phase morphology of the surface for elongated specimens, the specimens were immersed in hot xylene for 20 min to etch away the matrix, PE.

3. Results and discussion

3.1. Stress-strain behavior of injection molded PET/PE and PC/PE blends

Engineering stress-strain curves of PET/PE and PC/PE specimens measured at crosshead speeds of 50 mm/min

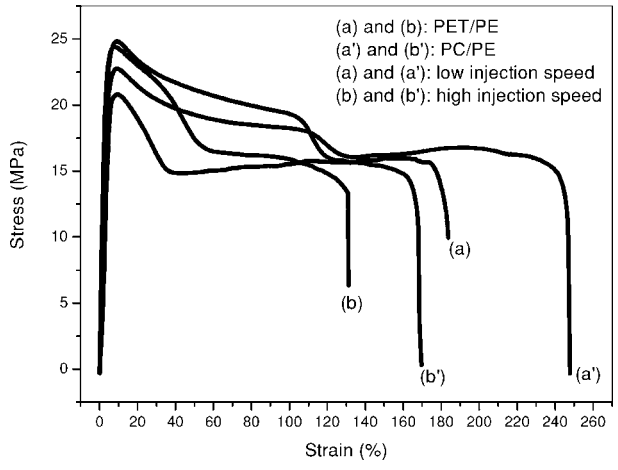

Figure 1 Typical stress-strain curves of PET/PE and PC/PE blends injection molded at different speed: (a) PET/PE, 10.0 mm/s; (a′): PC/PE, 10.0 mm/s; (b) PET/PE, 23.9 mm/s; (b′) PC/PE, 23.9 mm/s.

are shown in Fig. 1. In all cases, tensile stress showed a definite upper yield point followed by a stress drop, with completely different subsequent yielding and cold drawing. For PET/PE blend, the specimens obtained by both injection rates had similar stress-strain behavior except for the ultimate elongation. After yielding, the stress dropped rapidly to a constant that was maintained during the following cold drawing (necking extension). Finally, the specimens fractured in a tough manner without strain-hardening behavior. On the other hand, for the PC/PE blend, it is interesting that all specimens showed apparently two yielding zones. In the beginning, the common yielding occurred after some elastic deformation. The stress first dropped as quickly as for the PET/PE blend, then continued to drop slowly while the strain continued to increase substantially. When the elongation reached a certain point, the stress began to drop rapidly again, indicating a second yielding. Thereafter, the stress remained constant until the specimens were fractured.

All the injection molded PC/PE blend bars experienced twice apparent yielding. However there were considerable scatter about the ultimate elongations within samples as shown in Fig. 2, varying from 100 to 400%, with an average of 200% or so. It is interesting that except for only a slight increase with ultimate elongation, the second yielding began at an elongation about 100 to 150% regardless of the ultimate elongation.

The tensile properties including tensile strength, tensile modulus and ultimate elongation obtained from the stress-strain curves are listed in Table I. As shown in Fig. 2, the tensile strength and modulus for different specimens showed good repeatability, whereas the elongation at break scattered considerably. Considering the large scattering of the ultimate elongation, more than ten specimens were tested and the average value was reported. The following conclusions were drawn from Table I:

(1) For the same blend, the specimens injection molded at high injection speed have a slightly bit higher tensile strength and modulus than those molded at low injection speed, indicating that the higher melt flow rate in injection molding operation can, to some degree, enhance the mechanical properties of the parts.

(2) The reinforcement effect of PC to PE matrix was a little more noticeable than PET to PE though both blends were thermodynamically immiscible and technologically incompatible.

(3) The PET/PE blend had lower ultimate elongation than the PC/PE blend. And for the same blend system, the specimens molded at low injection rate had higher

TABLE I Tensile strength and tensile modulus of PET/PE and PC/PE blends injection molded at different injection speeds

	Tensile strength (MPa)	Tensile modulus (MPa)	Ultimate elongation (%)
PET/PE blend			
Low injection speed (10 mm/s)	23.3	940	190
High injection speed (23.9 mm/s)	24.2	1060	140
PC/PE blend			
Low injection speed (10 mm/s)	24.5	1100	240
High injection speed (23.9 mm/s)	25.5	1240	220

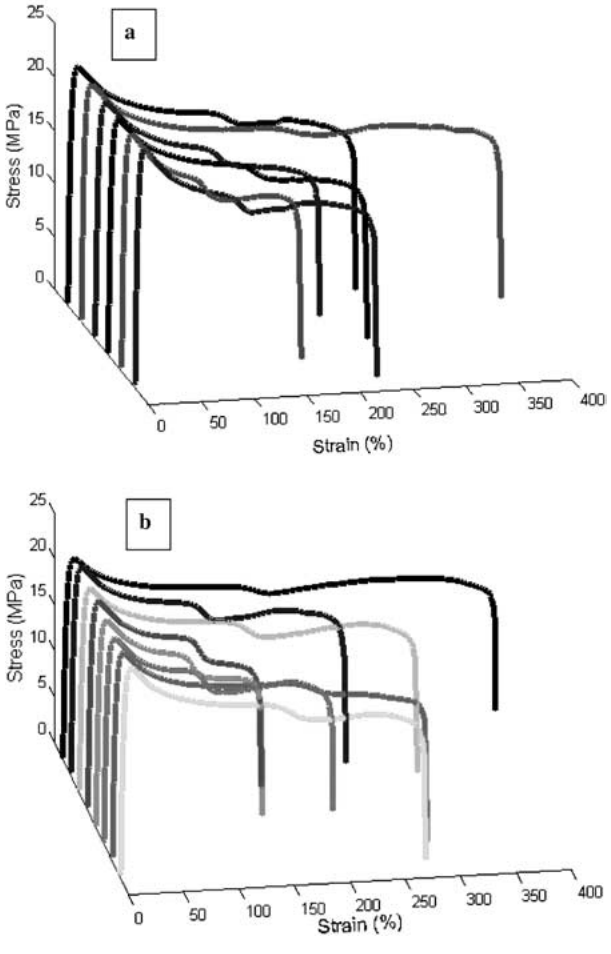

Figure 2 Stress-strain curves of PC/PE blends injection molded at different speed: (a) molded at 10.0 mm/s; (b) molded at 23.9 mm/s.

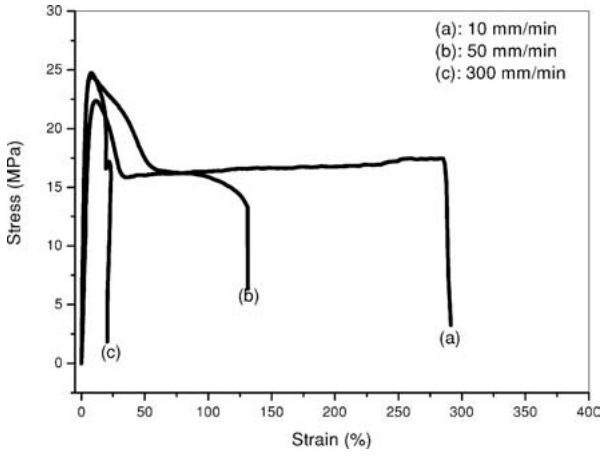

(a)

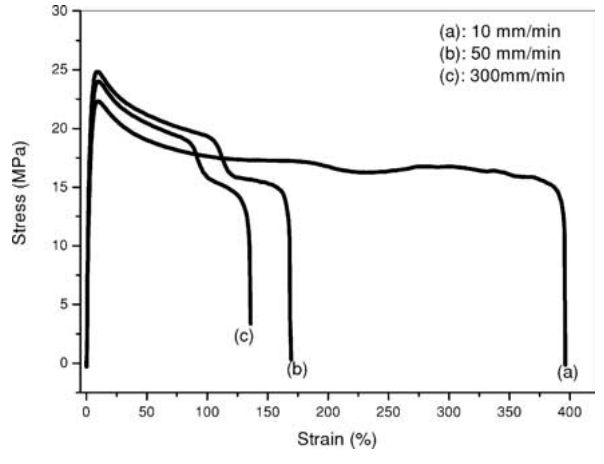

(b)

Figure 3 Influence of cross head speed on stress-strain behavior of PET/PE and PC/PE blends injection molded at 23.9 mm/s. (a) PET/PE blend and (b) PC/PE blend.

ultimate elongation than those molded at high injection rate. This is natural that the polymer chains in the part molded at lower rate were less oriented than those in the part molded at higher speed.

Fig. 3 presents the influence of crosshead speed on the stress-strain behavior of PET/PE and PC/PE blends injection molded at low rate. The stress-strain of both blends was crosshead speed-dependent. The tensile strength and modulus increased, and the elongation at break decreased with the increase of crosshead speed. For the PC/PE blend, the second yielding was less obvious for lower crosshead speed, but it was still visible. It is interesting that for the PC/PE blend, with the increase of crosshead speed, the length of the second cold drawing zone reduced considerably, while that of the first cold drawing zone generally had only a little decrease.

3.2. Morphology of stretched PET/PE and PC/PE blends

In paper I [29], the detailed gradient morphology (the skin-core structure) of the injection molded PET/PE and PC/PE blends is reported. Here, the morphology of the injection molded specimens after stretching was examined by SEM micrographs. Only the result of core zone with spherical particles in the original specimens is reported because the structure of the elongated phase in the sub-skin and intermediate layers was quite complicated and difficult to identify [30, 31]. Fig. 4 shows the morphology of the necked zone for the stretched PET/PE and PC/PE blends along the machine direction. Obvious debonding occurred between the dispersed PET particles and the matrix PE. The PET particles experienced slight plastic deformation, thus became ellipsoids with the long axis parallel to the machine direction. Additionally, there was apparent slippage at the interface between the PET particles and the PE matrix, resulting in voids behind the particles, and also large grooves where the PET particles were enveloped. For the PC/PE blend, the morphology in the core zone along the machine direction at 34%, 92% and ultimate elongation, were examined. The PC particles in the core layer experienced considerable plastic deformation throughout the stretching. Consequently, most of PC particles in the fractured specimen were deformed into fibers. At 34% elongation, most particles experienced only slight plastic deformation and they were deformed into ellipsoids as observed in tensile fractured PET/PE blend, with a few large particles deformed into dog-bonelike rods. With the elongation increased to 92%, more particles were deformed into rods or fibers along the drawing direction. Finally, when the specimen was fractured, a great amount of microfibers with high aspect ratio was formed. On the other hand, there were some very fine particles with little deformation coexisting in the fractured specimen, demonstrating that very small particles were difficult to deform upon elongation. The influence of cross head speed on the plastic deformation of the PC particle is shown in Fig. 5. At the speed of 30 mm/min (comparatively low) and 300 mm/min (comparatively high), the deformation of the PC particles was relatively small. Most particles appeared to be ellipsoidal, and were encaged in the furrows of the highly deformed PE matrix. The morphology of the cold drawn zone for tensile fractured PC/PE blend is also shown here in Fig. 6. The matrix PE was etched away by hot xylene, so many fibers were exposed. All the fibers were sinuated indicating that they have experienced large plastic deformation. Additionally, it seemed that some were broken upon stretching.

3.3. Macroscopic morphology evolution of PET/PE and PC/PE blends upon stretching

Figs 7 and 8 present the macroscopic morphology evolution of tensile testing specimens at a cross-head speed of 50 mm/min at room temperature. Upon stretching, PET/PE and PC/PE blends showed quite different macroscopic morphology development as well as stress whitening in yielding and cold drawing. For the PET/PE blend, the yielding and necking first took place at one point close to the non-gate end of the specimen, and subsequently the necking (cold drawing) spread out uniformly from this point. The stress whitening only appeared at the yield point and the succeeding cold drawing zone. The specimens obtained by two groups

of injection molding parameters had similar stress whitening. On the other hand, for the PC/PE blend, the whole test zone of the specimens were first elongated and deformed without necking behavior. Then stress whitening appeared slowly and simultaneously covered almost the entire specimen. Subsequently necking began to appear near the non-gate end, and the cold drawing zone extended uniformly from this point. The breaking point of the specimens was random. The PC/PE specimens injection molded at both low and high injection speed exhibited similar macroscopic morphology development. It is interesting that the necking formation happened at the second yield stage, not at the first one.

3.4. Origin of tensile behavior for injection molded PET/PE and PC/PE blends

The results obtained above indicate that the tensile behavior of injection molded PET/PE blend was generally similar to the common blend, while injection molded PC/PE blend exhibited unusual stress-strain curves, neck formation as well as stress whitening upon elongation.

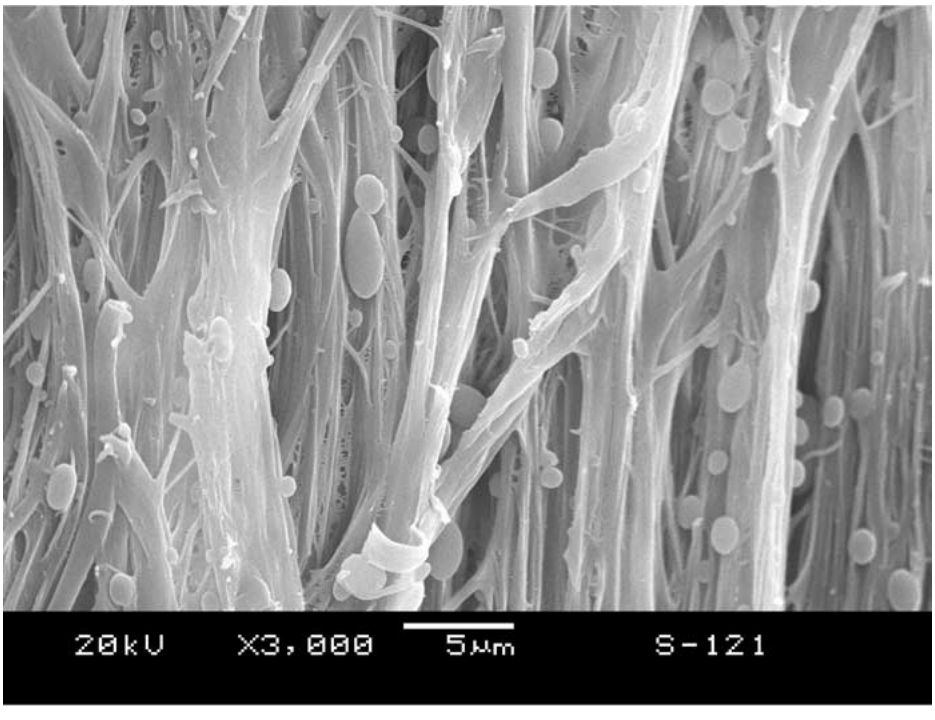

(a)

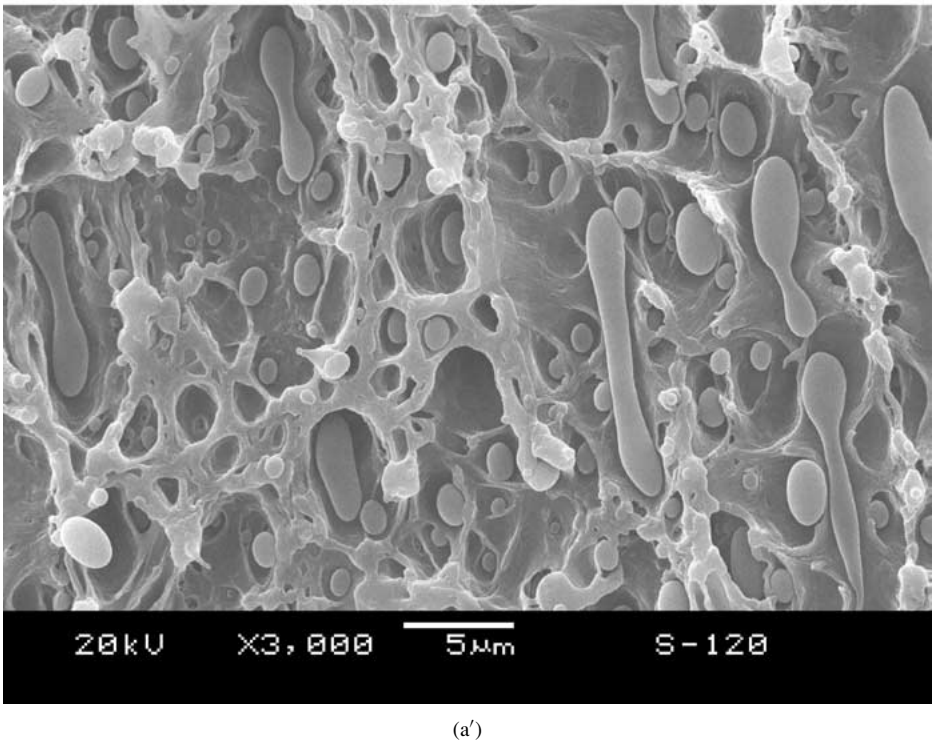

(a′)

Figure 4 SEM micrographs of injection molded PET/PE and PC/PE blends with different elongation: (a) PET/PE blend; (a′), (b′) and (c′) PET/PE blend; Elongation: (a′) 34%; (b′) 92%; (c′) and (a) ultimate (rapture). (*Continued*)

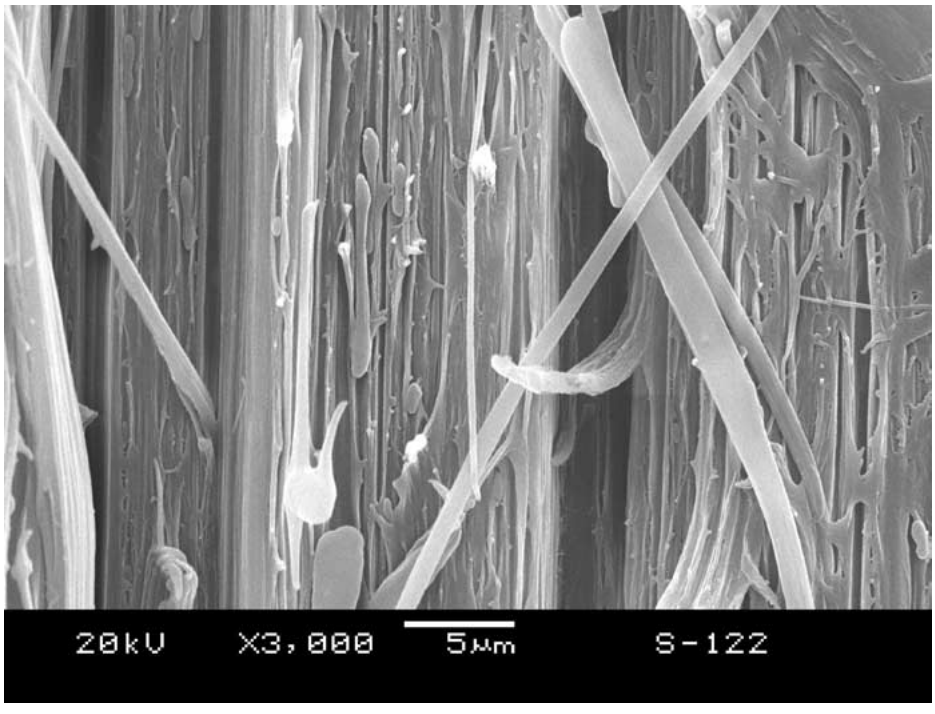

(b′)

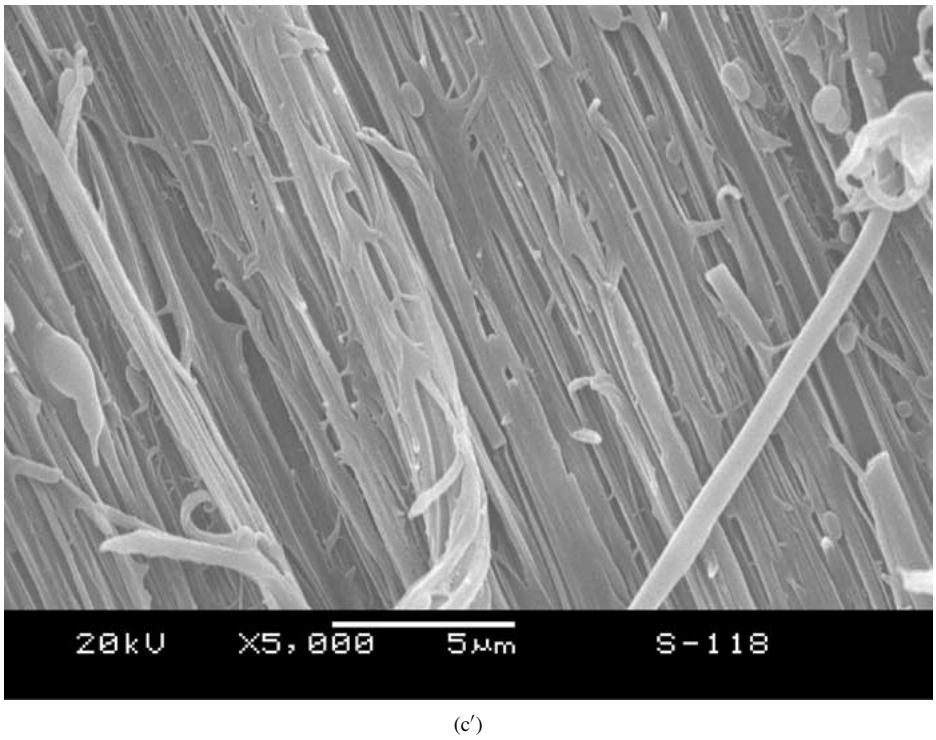

(c′)

Figure 4 (*Continued*).

As observed from the morphology of the as-injection molded PET/PE and PC/PE blends, both blends had skin-core structures [29]. In the sub-skin layer, there were more or less fibers. It was these *in situ* generated fibers that enhanced the tensile strength and modulus of the PET/PE and PC/PE blends. Fisa *et al*. [32] have compared the tensile mechanical properties of PP/PC blends obtained by injection molding and compression molding. Owing to flow induced dispersed phase orientation in injection molding, the tensile strength and modulus of the directly injection molded specimens were higher than those of compression molded specimens. In this study, when the melt flow rate was increased during injection molding, there were more highly elongated dispersed phase particles (sub-skin thickening). Therefore, it is reasonable that the tensile properties obtained at high injection speed were superior to the case at low injection speed. Moreover, the PC/PE blend has a little bit more noticeable reinforcement on the matrix PE than the PET/PE blend does though both blends are thermodynamically immiscible and technologically incompatible. This should be ascribed to the fact that PC/PE blend has relatively higher elongated orientation and a thicker sub-skin layer with fibrous structure, and the *in situ* fibers generated from the spherical particles in the core layer upon stretching.

In a previous study [33], the morphology-tensile mechanical properties of PET/PE and PC/PE blends with high interfacial bonding (pseudo-adhesion) were determined. It was found that in PC/PE blends numerous PC microfibers were formed *in situ*, while in PET/PE blends, slippage took place between the PET particles and the PE matrix, and hence PET particles exhibited only slight deformation. Consequently, PC had more pronounced reinforcement on PE than PET did. By calculation, the hydrostatic stress acting on PC particles upon stretching exceeded the yield strength of PC and thus PC particles underwent huge plastic deformation (fibrillation). Conversely, the stress on PET particles was lower than the yield strength of PET, thus only slight deformation occurred for the PET particles [34]. It seems that the same mechanism causes fibrillation of PC at an appropriate tensile rate as shown in Fig. 4 and hence more pronounced reinforcement on PE matrix.

The difference of macroscopic yielding deformation between the injection molded PC/PE blend and the PET/PE blend was caused by the different deformation mechanism upon elongation. For the PET/PE

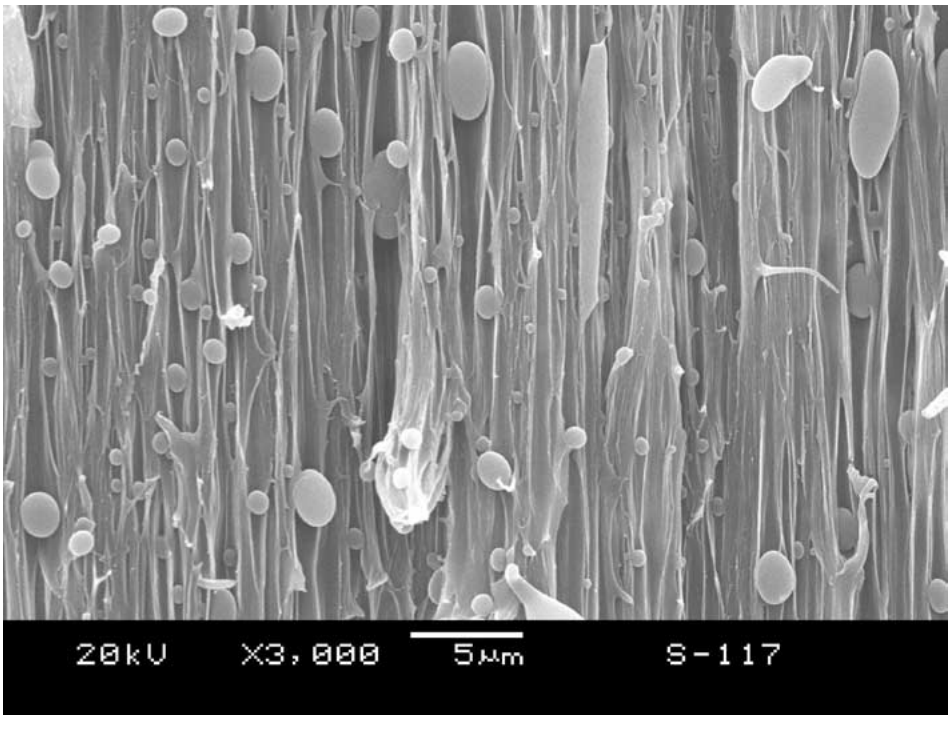

(a)

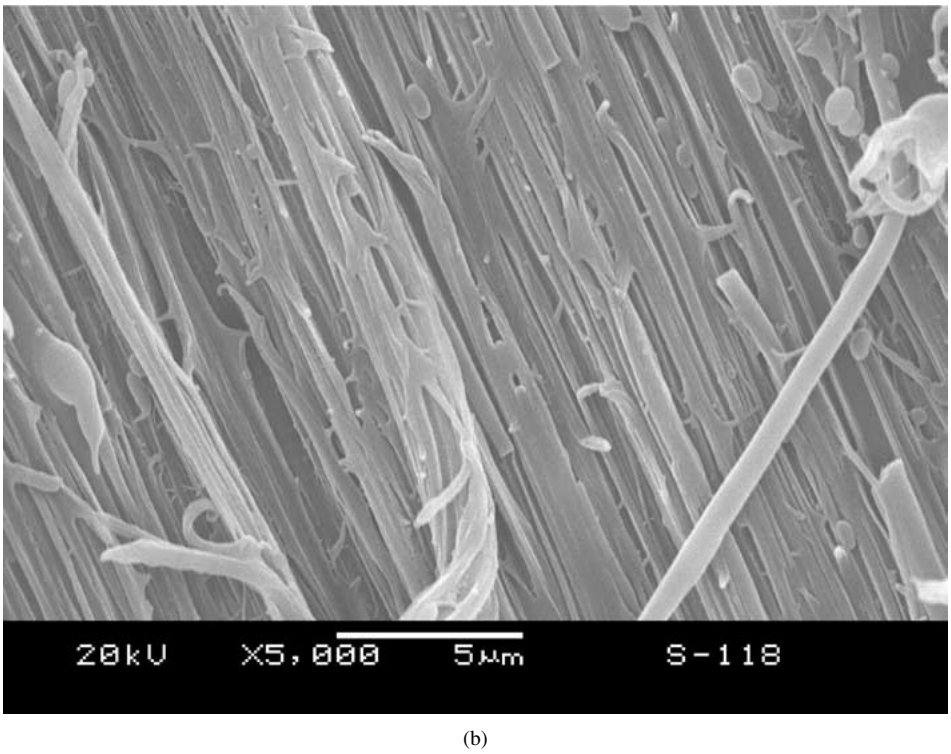

(b)

Figure 5 SEM micrographs of injection molded PC/PE blends tested at different cross head speed: (a) 30 mm/min, (b) 50 mm/min, and (c) 300%. (*Continued*)

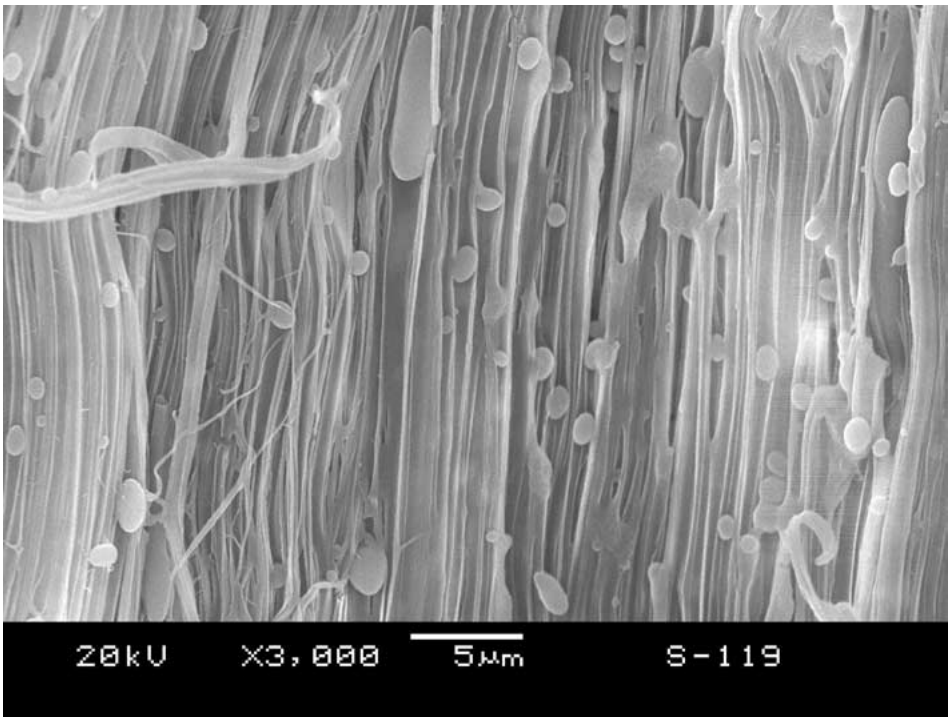

(c)

Figure 5 (*Continued*).

Figure 6 SEM micrograph of the surface of stretched PC/PE blend specimen etched by hot xylene.

blend, macroscopic deformation first took place on a weak point in the specimen, and the dispersed particles also underwent deformation. Because of the poor compatibility between PET and PE, debonding and slippage occurred at their interfaces, and hence small deformation occurred for PET particles. The elongated PET particles in the sub-skin layer had some reinforcement on PE, but the reinforcement was very limited since only a very small proportion of the PET particles were elongated. The reinforcement of PET particles could not offset the decrease in hardness caused by local temperature rise during stretching. The deformation continued from the weak point and propagated from this zone, followed by regular necking formation and cold drawing phenomenon. Due to interfacial slippage between PET particles and PE matrix, grooves and voids were formed, and cavitation occurred. Therefore, the necking and cold drawing were accompanied by stress whitening in the deformed zone.

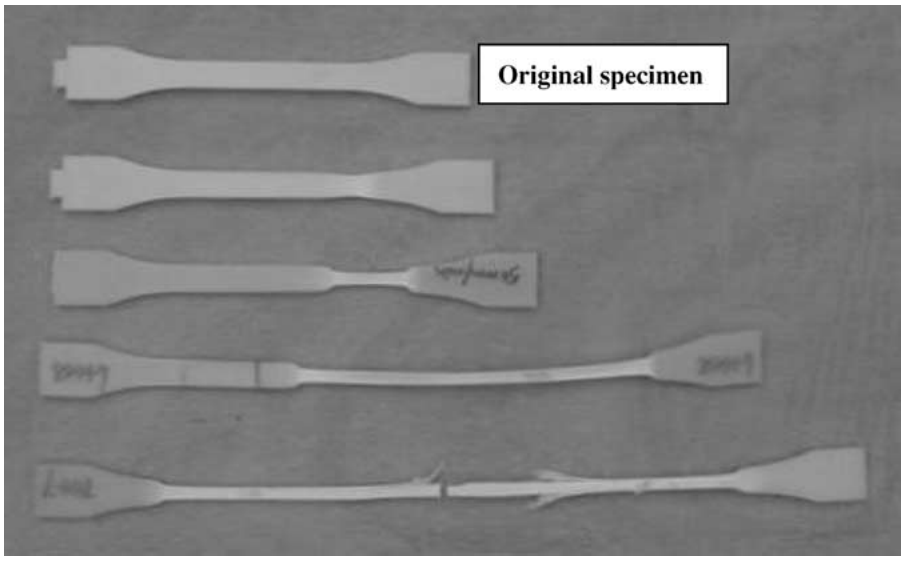

Figure 7 Macroscopic morphology evolution of injection molded PET/PE blend specimen during elongation.

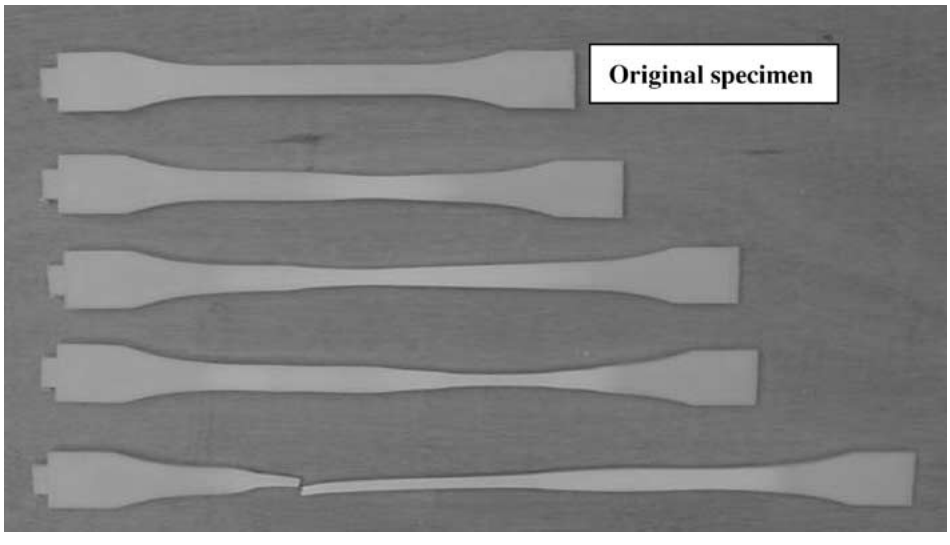

(a)

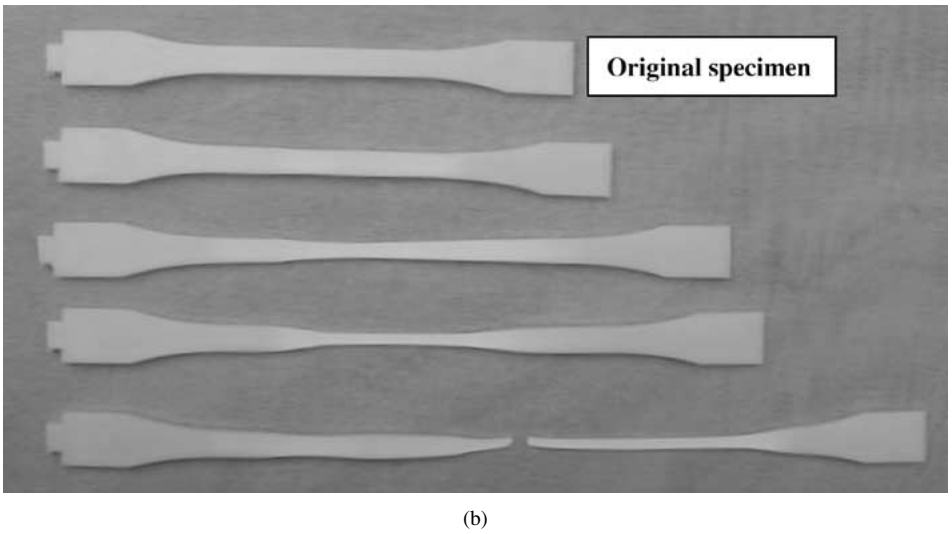

(b)

Figure 8 Macroscopic morphology evolution of injection molded PC/PE blend specimen during elongation: (a) low injection speed and (b) high injection speed.

For the PC/PE blend, owing to comparatively higher concentration of injection induced fibers that distributed and transferred the external stress, the specimen first deformed evenly in the entire tested zone, and after the first yielding, the stress dropped slowly while the elongation continued. Due to the incompatibility between PC and PE, the interfaces debonded to some degree, and cavitation occurred causing the

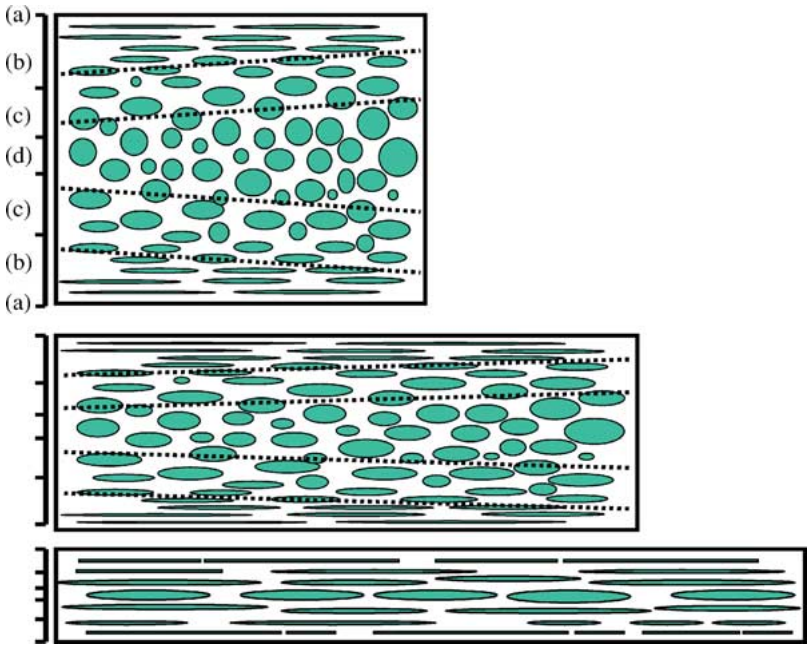

Figure 9 Macroscopic morphology evolution of injection molded PC/PE blend specimen during elongation: (a) low injection speed and (b) high injection speed.

stress whitening over the entire specimen. However, the debonding is minor compared to that in the PET/PE blend because of the limitation of the fibers in the sub-skin layer. When the elongation reached a certain value, the fibers in the sub-skin layer would no longer endure the external stress and then failure occurred. The second yield and necking took place when the load dropped quickly to a constant value. Hereafter, the strain continued to increase until the specimen was broken.

The typical deformation and fibrillation process of PC/PE blend upon elongation was presented in Fig. 9. The fibers formed in the subskin layer during injection molding were stretched and developed into finer fibers, while the spherical or ellipsoidal particles were plastically deformed into rods, and even fibers at very high elongation. That is why the fibers on the cold zone surfaces were sinuous (Fig. 6), indicating that these fibers experienced plastic deformation. The deformation of PET/PE blends upon elongation was also schematically presented in Fig. 10. The former elongated PET particles might be further drawn and became finer upon stretching like PC fibers while the spherical particles in the core zone only experienced slight deformation to form ellipsoids. The slippage between PET particles and PE matrix resulted in various grooves.

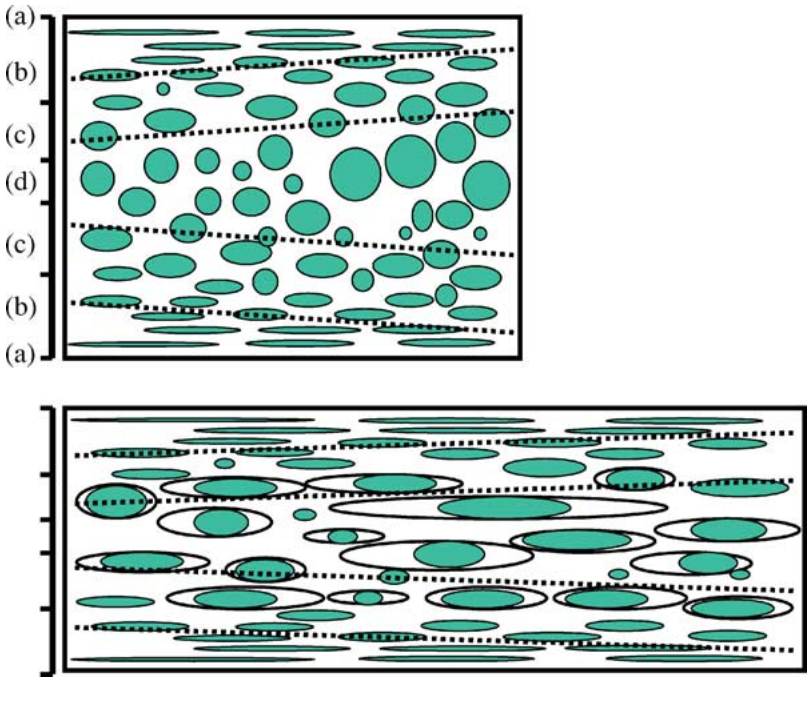

Figure 10 Schematic representation for the typical deformation and fibrillation process of PET/PE blend upon elongation: (a) surface, (b) sub-skin layer, (c) intermediate layer, and (d) core zone.

4. Conclusions

(1) For the same blend, the specimens injection molded at higher injection speed had slightly higher tensile strength and modulus than those made at lower injection speed. The reinforcement effect of PC to PE matrix was more noticeable than PET to PE. The ultimate elongation of the PET/PE blend was lower than that of the PC/PE blend.

(2) For the stress-strain behavior, while the PET/PE blend behaved like a common injection-molded immiscible blend, the PC/PE blend unusually exhibited two yielding stages. The ultimate elongation of the PC/PE blend scattered noticeably, the second yielding began to appear at an elongation ranging from 100 to 150%. Samples stretched at lower crosshead speed showed less obvious second yielding. With the increase of crosshead speed, the length of the second cold drawing zone reduced considerably, while that of the first cold drawing zone had only a little decrease.

(3) For the PET/PE blend, obvious debonding between the dispersed PET particles and the matrix PE occurred upon stretching, resulting in voids behind the particles and also large grooves. The PET particles experienced slight plastic deformation to form ellipsoids. For the PC/PE blend, the PC particles in the core layer of the specimen experienced considerable plastic deformation throughout the tensile test. Consequently, most of PC particles in the fractured specimen were deformed into fibers.

(4) Owing to comparatively high concentration of injection-induced fibers that can average or transfer the external stress, the specimens made from the PC/PE blend first deform evenly in the entire tested zone, and after the first yielding, the stress decreases slowly while the strain extends. When the elongation arrives at a certain value, the fibers in the sub-skin layer cannot endure the external stress, and accordingly the second yield takes place. From the macroscopic view, the second yield and necking take place while the load drops quickly to a constant value.

Acknowledgements

The authors gratefully acknowledge the financial support of this work by the Nature Science Foundation of China (grant: 50103007). We also heavily indebted to Miss Xin-Yuan Zhang and Mr. Zhu Li from Center of Analysis and Test of Sichuan University for careful SEM observation.

References

1. J. KARGER-KOCSIS and I. CSIKAI, *Polym. Eng. Sci.* **27** (1987) 241.
2. C. D. HAN, K. U. KIM, J. PARKER, N. SISKOVIC and C. R. HUANG, *Appl. Polym. Symp.* **20** (1973) 91.
3. R. C. THAMM, *Rubber Chem. Technol.* **50** (1977) 24.
4. W. J. HO and R. SALOVEY, *Polym. Eng. Sci.* **21** (1981) 839.
5. R. E. SKOCHDOPOLE, C. R. FINCH and J. MARSHALL, *ibid.* **27** (1987) 627.
6. B. D. FAVIS, in "Polyemr Blends Volume 1: Formulation," edited by D. R. Paul and C. D. Bucknall (John Wiley & Sons, New York, 2000) p. 502.
7. F. GHIAM and J. L. WHITE, *Polym. Eng. Sci.* **31** (1991) 76.
8. M. P. LEE, A. HILTNER and E. BAER, *Polymer* **33** (1992) 675.
9. *Idem.*, *ibid.* **33** (1992) 685.
10. L. DORAZIO, C. MANCARELLA, E. MARTUSCELLI, G. STICOTTI and G. CEDDHIN, *ibid.* **72** (1999) 701.
11. Y. SON, K. H. AHN and K. CHAR, *Polym. Eng. Sci.* **40** (2000) 1385.
12. B. D. FAVIS, in "Polyemr Blends Volume 1: Formulation," edited by D. R. Paul and C. D. Bucknall (John Wiley & Sons, New York, 2000) p. 502.
13. B. D. FAVIS and J. P. CHALIFOUX, *Polymer* **29** (1988) 1761.
14. C. M. HSIUNG, M. CAKMAK and Y. ULCER, *ibid.* **37** (1996) 4555.
15. M. N. BUREAU, E. D. FRANCESCO, J. DENAULT and J. I. DICKSON, *Polym. Eng. Sci.* **39** (1999) 1119.
16. J. KARGER-KOCSIS and D. E. MOUZAKIS, *ibid.* **39** (1999) 1365.
17. G. GUERRICA-ECHEVARRIA, J. I. EGUIAZABAL and J. NAZABAL, *J. Appl. Polym. Sci.* **72** (1999) 1113.
18. M. N. BUREAU, H. EI KADI, J. DENAULT and J. I. DICKSON, *Polym. Eng. Sci.* **37** (1997) 377.
19. B. OHLSSON and B. TONELL, *ibid.* **38** (1998) 108.
20. K. W. MCLAUGHLIN, *ibid.* **29** (1989) 1560.
21. L. D'ORAZIO, C. MANCARELLA, E. MARTUSCELLI, G. CECCHIN and R. CORRIERI, *Polymer* **40** (1999) 2745.
22. G. GUERRICA-ECHEVARRIA, J. I. EGUIAZABAL and J. NAZABAL, *Polym. Compos.* **21** (2000) 864.
23. S. K. PAL and D. D. KALE, *J. Polym. Res.* **7** (2000) 107.
24. B. OHLSSON and B. TORNELL, *Polym. Eng. Sci.* **38** (1998) 108.
25. L. DORAZIO and G. CECCHIN, *Polymer* **42** (2001) 2675.
26. B. NYSTEN, A. GHANEM, J. L. COSTA and R. LEGRAS, *Polym. Intern.* **48** (1999) 334.
27. Y. G. SON and K. CHAR, *SPE ANTEC Conf. Proc.* **3** (1996) 2668.
28. Y. D. WANG and M. CAKMAK, *ibid.* **2** (1996) 1581.
29. Z. M. LI, W. YANG, S. Y. YANG, B. H. XIE, R. HUANG, M. B. YANG and J. M. FENG, *Paper I: J. Mater. Sci.*, this issue.
30. S. FELLAHI, B. D. FAVIS and B. FISA, *Polymer* **37** (1996) 2615.
31. B. FISA, B. D. FAVIS and S. BOURGEOIS, *Polym. Eng. Sci.* **30** (1990) 1051.
32. S. FELLAHI, B. D. FAVIS and B. FISA, *SPE ANTEC Tech. Pap.* **39** (1993) 211.
33. Z. M. LI, X. R. FU, M. B. YANG, B. H. XIE, R. HUANG and J. M. FENG, *J. Mater. Sci. Lett.* **21** (2002) 1063.
34. Z. M. LI, X. R. FU, M. B. YANG, B. H. XIE, R. HUANG and J. M. FENG, *Polym. Eng. Sci.*, in press.

Received 18 July
and accepted 14 August 2003